Laser and Particle Beams (2012), *30*, 313–317.

doi:10.1017/S0263034612000080

Diagnosis of the soft X-ray spectrum emitted by laser-plasmas using a spectroscopic photon sieve

YULIN GAO,[1] WEIMIN ZHOU,[1] LAI WEI,[1] LEIFENG CAO,[1] XIAOLI ZHU,[2] ZONGQING ZHAO,[1] YUQIU GU,[1] BAOHAN ZHANG,[1] AND CHANGQING XIE[2]

[1]National Key Laboratory of Laser Fusion; Research Center of Laser Fusion, Mianyang, Sichuan, China
[2]Institute of Microelectronics, Chinese Academy of Sciences, Beijing, China

(Received 15 November 2011; Accepted 26 January 2012)

Abstract

Laser plasma experiments, which demonstrated the single order diffraction property of spectroscopic photon sieve (a novel single-order diffraction grating), were performed on the SILEX-I femto-second laser facility. High-intensity laser radiation was focused onto a Cu target to generate plasma. The spectra of soft X-ray from copper plasmas have been measured with spectroscopic photon sieve based spectrograph. The results show that the spectroscopic photon sieve is able to provide soft X-ray spectrum free from higher-order diffraction components. The measured spectra obtained with such a spectroscopic photon sieve need no unfolding process to extract higher-order diffraction interference.

Keywords: Higher-order diffraction; Laser plasma interaction; Soft X-ray spectrum; Spectroscopic photon sieve; Transmission grating

INTRODUCTION

Diagnoses of soft X-ray spectra emitted by laser-produced plasmas are of vital importance both to research and in applications involving laser-driven inertial confinement fusion (Hogan *et al.*, 1992), soft X-ray lasing in plasmas produced from solid targets (Nagata *et al.*, 1993; Ditmire *et al.*, 1995), gas puff targets (Fiedorowicz *et al.*, 1996), and coherent extreme-ultraviolet (XUV) radiation through high-order-harmonic generation (Huillier & Balcou, 1993; Ditmire *et al.*, 1995; Miyazaki & Takada, 1995). There are various diffraction elements for dispersing soft X-rays, for example, crystal (Koenig *et al.*, 1997; Arora *et al.*, 2000), grazing grating (Chowdhury *et al.*, 1999), or transmission grating (Fiedorowicz *et al.*, 1996). Although crystal spectrographs based on Bragg reflection and flat field grating spectrographs based on Rowland circle geometry can be used to achieve high spectral resolution, these are quite cumbersome in operation and require critical alignment. In contrast, transmission grating spectrographs (TGS) operating at normal incidence are convenient to use and can be coupled to detectors such as microchannel plates (MCPs) and charge-coupled-device (CCD) cameras for online monitoring (Fiedorowicz *et al.*, 1996; Alexandrov *et al.*, 1988; Zeng *et al.*, 1992) and streak cameras for temporally resolved measurements (Fiedorowicz *et al.*, 1996; Bourgade *et al.*, 1988; Sigel *et al.*, 1992). As a matter of fact, TGS have been widely used in laser-plasma studies requiring a wide spectral range (0.5 nm–20 nm), and a moderate resolution (Fiedorowicz *et al.*, 1996; Alexandrov *et al.*, 1988; Eidmann *et al.*, 1986; Bourgade *et al.*, 1988; Zeng *et al.*, 1992; Sigel *et al.*, 1992). However, the so-called black-white transmission gratings, which have been presently used in soft X-ray spectroscopy studies (Fill *et al.*, 1999; Yang *et al.*, 2003), have inherent higher-order diffractions (Born & Wolf, 1999). Furthermore, the diffractions from various orders may overlap one with others and a complex unfolding process is necessary to extract the usable first-order diffraction (Schriever *et al.*, 1997; Yang *et al.*, 2003; Eagleton & James, 2004).

Recently, some new gratings, which can suppress higher-order diffraction components, have been developed in the X-ray region, such as binary sinusoidal transmission grating (Cao *et al.*, 2007), and quantum-dot-array diffraction grating (Wang *et al.*, 2007, 2008; Kuang *et al.*, 2010, 2011). A novel two-dimensional (2D) diffraction grating, called a spectroscopic photon sieve (SPS), has been developed (Cao *et al.*, 2011). By distributing a large number of pinholes on an aurum substrate, the SPS can be free-standing while suppress

Address correspondence and reprint requests to: Leifeng Gao, National Key Laboratory of Laser Fusion, Research Center of Laser Fusion, China Academy of Engineering Physics, P.O. Box, 919-986-6, Mianyang, Sichuan Province, China. E-mail: liaode_2002@yhaoo.com.cn

higher-order diffraction components. Using electron-beam lithography, a SPS of a spatial frequency (1000 line/mm) has been designed and fabricated for the first time (Cao *et al.*, 2011).

In this paper, the first experiments demonstrating the single-order diffraction property of a SPS are described. Compared with spectra of ordinary transmission grating, spectra from SPS are free from higher-order diffraction components, and as a consequence no complex unfolding processes are needed to eliminate higher-order-diffraction interference.

EXPERIMENT

A schematic of the experimental set-up is shown in Figure 1. Plasma was produced by irradiating planar solid strips of copper with laser pulses of 5 J energy in 30 fs (FWHM) duration from a Nd: glass laser system ($\lambda_L = 800$ nm) at an angle of 21° to the target incident normal. An $F/2.625$ off-axis parabolic mirror of 420-mm focal length focused the laser beam on the target to a focal spot diameter of 35 μm as measured from X-ray pinhole pictures of the plasma emissions. The target chamber was evacuated to 10^{-4} Torr, and the target was moved after each laser shot to provide a fresh surface for plasma production.

Soft X-ray emission spectra from the plasmas were recorded by a TGS viewing the X-ray emission in a direction perpendicular to the main laser. This spectrograph consisted of a SPS of 1000 nm, and an X-ray CCD camera with 2048 × 2048 array of 13.5 μm × 13.5 μm pixels was used to provide relatively time-integrated spectra. This SPS, with a rotund cross-section of diameter of 80 μm, was mounted at a distance of 1000 mm from the target. The diffracted radiation was recorded with an X-ray CCD camera placed at a distance of 500 mm from the SPS. Using these distance settings, this spectrograph based covered a broad spectral range (3–200 Å) with a resolution of about 2.8 Å at λ = 13Å (Sailaja *et al.*, 1998).

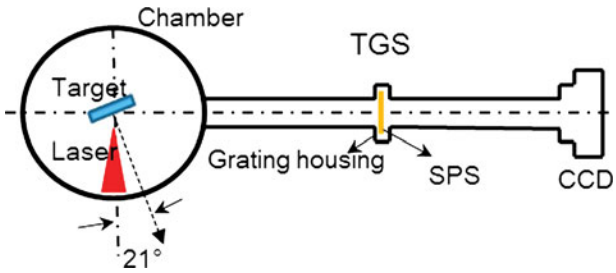

Fig. 1. (Color online) A schematic of the experiments.

Figure 2a shows the schematic structure of a SPS. The thin substrate, from X-ray opaque material such as gold, is cut uniformly into $N \times N$ small squares with side length denoted by d, and from within each square is drilled out at random positions a circular hole of a certain diameter, denoted by a, to enable X-rays to be transmitted. Along the x- and y-axes, the pinholes have a quasi-sinusoidal distribution. Generally, the diameter of these holes (a) is chosen to be half the side length (d). The structural figure of the SPS is designed by computer and fabricated in the grating material using electron beam lithography (Anderson *et al.*, 2000), which is controlled by computer to make the design to be reproduced in the grating material. A microstructure of a SPS used in experiments is shown in Figure 2b. With a gold substrate thickness of 400 nm, the period of this SPS is 1000 nm and hole diameters are nearly 500 nm.

By fast Fourier transform techniques, the diffraction pattern of the SPS can be easily obtained. Table 1 lists the numerical simulation parameters consistent with the SPS used in this experiment. Figure 3 shows the far-field diffraction pattern and the intensity profile of the SPS of 1000 lines/mm at the incident wavelength of 1 nm. The middle peak of the maximum intensity in Figure 3a is the zero-order diffraction, and the others are all first-order diffractions. According to the intensity profile seen in Figure 3b, the relative diffraction efficiency (energy ratio of first-order diffractions to zero-order diffraction) is about 21%. At the same time, the higher-order diffraction components are significantly suppressed, which are only about 0.22% of the first-order diffractions and could be as low as the background radiation noise of the CCD. So a clear spectrum without higher-order diffractions may be obtained by the SPS for the X-ray measuring in laser plasma experiments.

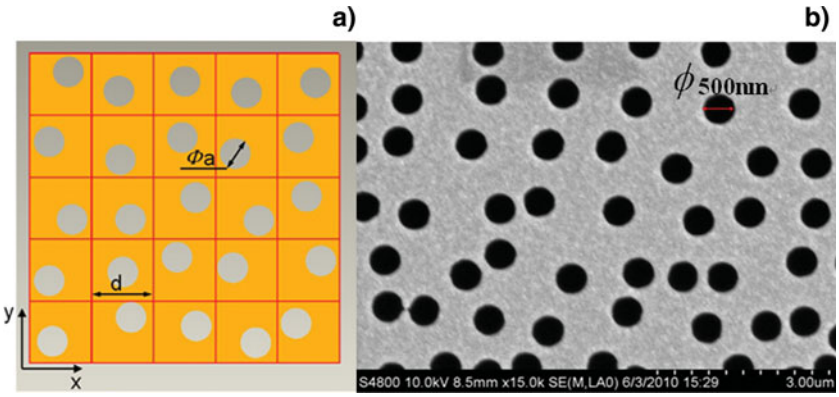

Fig. 2. (Color online) (**a**) A schematic structure of the SPS. The grating period is d and the diameter of the pinhole $a = d/2$. (**b**) A microstructure of the SPS with a spatial frequency of 1000 lines/mm corresponding $d = 1$ μm.

https://doi.org/10.1017/S0263034612000080 Published online by Cambridge University Press

Table 1. *Parameters used in the process of simulating the diffraction pattern of the SPS*

Incident Wavelength λ (nm)	Period d (μm)	Diffraction distance Z (m)	Pixel of CCD Δx (μm)	CCD array
1	1	1.22	20	500 × 500

RESULTS AND DISCUSSION

The X-ray emission spectrum was recorded in a direction perpendicular to the main laser, as shown in Figure 1. X-ray emission spectrum images for copper plasma were obtained by the X-ray CCD at laser energy of 3.1 J. As expect, there were nine strong diffraction peaks in Figure 4a. The center peak was the zero-order diffraction with the highest brightness; other peaks were diffracted symmetrically about the central peak. A plot of optical density versus wavelength of the X-ray spectral lines along the X-axis is given in Figure 4b. Two pairs of diffractions with different optical densities appear symmetrically on either side of the zero-order diffraction. Following the data described in the X-ray handbook, we have identified and classified these copper spectral lines as belonging to the electron transitions of the L- and M-band neon-like ions over wavelengths ranging from 1.1 to 10 nm. The L-band was resulted from electronic transitions from the L-shell in copper ions and the M-band was from the M-shell electronic transitions. The X-ray continuum was primarily emitted near the surface of the target. If there was an increase of the intensity of the laser irradiation, there would have been a stronger intensity of the L-band from the copper plasma soft X-ray radiation. Besides the first-order diffractions, none higher-order diffraction of the L- and M-band was found in the X-ray spectral lines. Due to environmental noise and background radiation noise of CCD, the relative diffraction efficiency of the first L-band intensity to the zero-order peak 26.02% was somewhat higher than that of numeric simulation 21%.

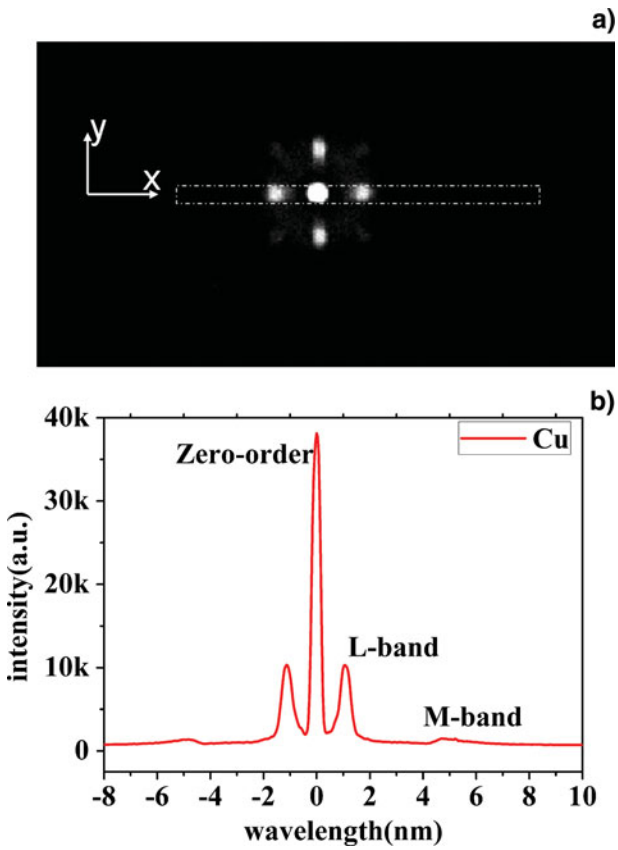

Fig. 4. (Color online) A typical X-ray emission spectrum of copper plasma at a laser energy of 3.1 J: (**a**) Spectrum image recorded by an X-ray CCD; (**b**) The optical density of the recorded soft X-ray spectrum along the x-axis in Figure 4a.

The intensity profiles of emission spectra measured by the different dispersive elements are shown in Figure 5, and the intensity is peak-normalized to 1 in their first L-band. The blue profile represents the X-ray emission spectrum of

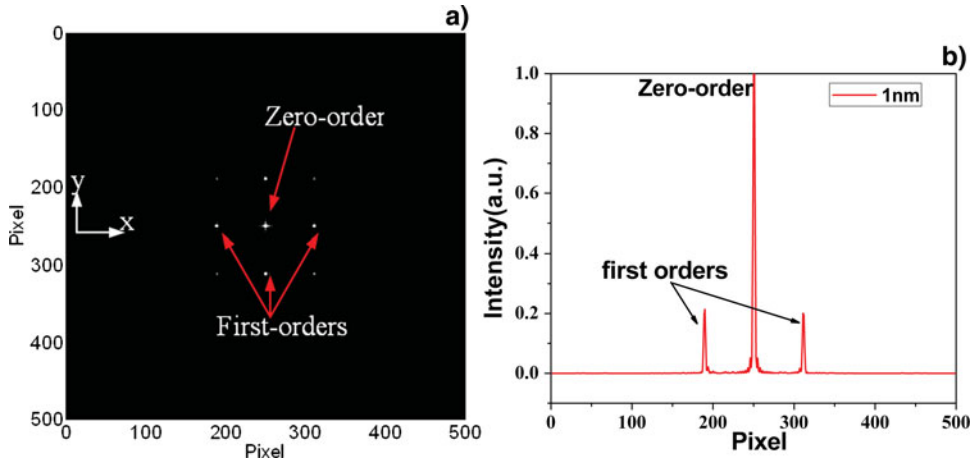

Fig. 3. (Color online) (**a**) Calculated far-field diffraction pattern for the SPS at 1nm wavelength. (**b**) Profile across the *x*-axis in Figure 3a.

https://doi.org/10.1017/S0263034612000080 Published online by Cambridge University Press

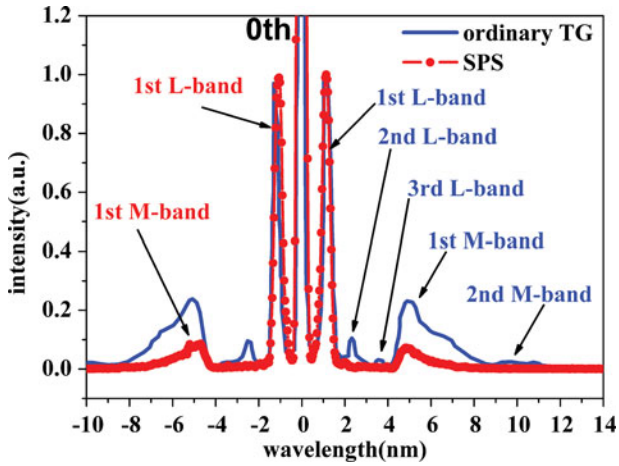

Fig. 5. (Color online) Contrast of copper plasma emission spectrum measured by the SPS and ordinary transmission grating.

copper plasma measured using an ordinary transmission grating at laser energy of 50 mJ from a 3 TW laser device (Liu *et al.*, 1999), and the red profile represents the emission spectrum measured by a SPS at laser energy of 3.1 J with a 100 TW laser device. Obvious L- and M-band emissions, corresponding to energy ranges 900 eV–1.1 keV and 250 eV–300 eV, respectively, were found in both line spectra. Besides the first-order diffractions, the secondary-order diffractions of the M-band, as well as the secondary-order and tertiary-order launch spectrum diffraction signals of the L-band, were found in the spectrum line of the ordinary transmission grating. And the fourth-order of the L-band overlay the first-order of M-band launch spectrum. Thus a complex unfolding process must be done to subtract the higher-order-diffraction contributions in order to obtain well resolved spectrum. In contrast the red profile provides a clean and direct spectrum, only first-order of the L-band and M-band diffractions exist, and all higher-order diffractions are almost completely inhibited.

Except for the difference in higher-order diffractions, the relative intensity of the M-band emission with an ordinary transmission grating is higher than that of the SPS. This is due to the difference in laser energy, 3.1 J of laser energy for SPS experiment and 50 mJ of laser energy for the transmission grating experiment. With increased laser energy, the target surface intensity is much higher, and the plasma temperature is higher also. Thus the L-band has been proportionately enhanced.

CONCLUSION

Using a SPS instead of an ordinary transmission grating, we measured the spectrum from copper plasma produced by a high intensity laser interacting with the plane copper target. Compared with soft X-ray spectroscopy using an ordinary transmission grating, spectroscopy with a SPS is more clean and direct, and a complex unfolding process to eliminate higher-order-diffraction interference is not required. With absolute diffraction efficiency for the SPS and quantum efficiency for the X-ray CCD, an absolute spectral analysis of soft x-ray emissions from laser-produced plasma could be done.

ACKNOWLEDGMENTS

This work was supported by the National Natural Science Foundation of China (No. 10727504), and the Development Foundation of China Academy of Engineering Physics (No. 2011B0102022). The authors gratefully acknowledge Professor Jiyan Zhang and Professor Mingqi Cui for their useful discussion.

REFERENCES

Alexandrov, Yu.M., Koshevoi, M.O., Murashova, V.A., Nikitina, T.F., Rupasov, A.A., Sklizkov, G.V., Shikanov, A.S., Yakimenko, M.N., Zakharenkov, Yu.A., Eidmann, K., Sigel, R. & Tsakiris, G.D. (1988). X-ray spectrometer using a free-standing transmission grating and a microchannel plate as detector for laser plasma studies. *Laser Part. Beams* **6**, 561–567.

Anderson, E.H., Olynick, D.L., Harteneck, B., Veklerov, E., Denbeaux, G., Chao, W., Lucero, L., Johnson, L. & Attwood, D. (2000). Nanofabrication and diffractive optics for high-resolution X-ray applications. *Vac. Sci. Technol. B.* **18**, 2970

Arora, V., Kumbhare, S.R., Naik, P.A. & Gupta, P.D. (2000). A simple high-resolution on-line X-ray imaging crystal spectrograph for laser-plasma interaction studies. *Rev. Sci. Instrum.* **71**, 2644–2650.

Born, M. & Wolf, E. (1999). *Principles of Optics: Electromagnetic Theory of Propagation, Interference and Diffraction of Light*. New York: Cambridge University Press.

Bourgade, J.L., Combis, P., Jacquet, M.L., Breton, J.P.L., Mascureau, J.D., Naccache, D., Sauneuf, R., Thiell, G., Keane, C., MacGowan, B. & Matthews, D. (1988). SPARTUVIX: A time-resolved XUV transmission grating spectrograph for x-ray laser research. *Rev. Sci. Instrum.* **59**, 1840.

Cao, L.F., Förster, E., Fuhrmann, A., Wang, C.K., Kuang, L.Y., Liu, S.Y. & Ding, Y.K. (2007). Single order X-ray diffraction with binary sinusoidal transmission grating. *Appl. Phys. Lett.* **90**, 053501.

Cao, L.F., Gao, Y.L., Zhou, W.M., Wei, L., Zang, H.P., Fan, W., Zhao, Z.Q., Gu, Y.Q., Zhang, B.H., Zhu, X.L., Xie, C.Q., Ye, T.C., Zhou, H.J., Huo, B.L. & Cui, M.Q. (2011). Single order spectra by disperse soft X-ray with spectroscopic photon sieve. *Opt. Expr.* (In press).

Chowdhury, A., Joshi, R.A., Kumnhare, S.R., Naik, P.A. & Gupta, P.D. (1999). Development of a flat-field XUV spectrograph for laser plasma interaction studies. *Sadhana.* **24**, 557–566.

Ditmire, T., Hutchinson, M.H.R., Key, M.H., Lewis, C.L.S., MacPhee, A., Mercer, I., Neely, D., Perry, M.D., Smith, R.A., Wark, J.S. & Zepf, M. (1995). Amplification of xuv harmonic radiation in a gallium amplifier. *Phys. Rev. A.* **51** R4337–R4340.

Eagleton, R.T. & James, S.F. (2004). Transmission grating streaked spectrometer for the diagnosis of soft x-ray emission from ultra-high intensity laser heated targets. *Rev. Sci. Instrum.* **75**, 3969.

Eidmann, K., Kishimoto, T., Herrman, P., Mizui, J., Pakula, R., Sige, R. & Witkowski, S. (1986). Absolute soft X-ray measurements with a transmission grating spectrometer. *Laser Part. Beams.* **4**, 521–530.

https://doi.org/10.1017/S0263034612000080 Published online by Cambridge University Press

Fiedorowicz, H., Bartnik, A., Szczurek, M., Fill, E., Li, Y.L. & Pretzier, G. (1996). XUV emission from an elongated plasma column produced using a high-power laser with a gas puff target. *Laser Part. Beams* **14**, 253–260.

Fill, E., Stephan, K.H., Predehl, P., Pretzler, G., Eidmann, K. & Saemann, A. (1999). Transmission grating spectroscopy in the 10 keV range. *Rev. Sci. Instrum.* **70**, 2597.

Hogan, W.J., Bangerter, R. & Kulcinski, G.L. (1992). Energy from Intertial Fusion. *Phys. Today* **45**, 42–50.

Huillier, A.L. & Balcou, P. (1993). High-order harmonic generation in rare gases with a 1-ps 1053-nm laser. *Phys. Rev. Lett.* **70**, 774–777.

Koenig, M., Boudenne, J.M., Legriel, P., Benuzzi, A., Grandpierre, T., Batani, D., Bossi, S., Nicolella, S. & Benattar, R. (1997). A computer driven crystal spectrometer with charge coupled device detectors for x-ray spectroscopy of laser plasmas. *Rev. Sci. Instrum.* **68**, 2387–2392.

Kuang, L.Y., Cao, L.F., Zhu, X.L., Wu, S.C., Wang, Z.B., Wang, C.K., Liu, S.Y., Jiang, S.E., Yang, J.M., Ding, Y.K., Xie, C.Q. & Zheng, J. (2011). Single-order diffraction transmission grating used in x-ray spectroscopy. *Opt. Lett.* **36**, 3954–3956.

Kuang, L.Y., Wang, C.K., Wang, Z.B., Cao, L.F., Zhu, X.L., Xie, C.Q., Liu, S.Y. & Ding, Y.K. (2010). Quantum-dot-array diffraction grating with single order diffraction property for soft x-ray region. *Rev. Sci. Instr.* **81**, 073508.

Liu, Y.Q., Zhang, L.Q., Song, X.Y., Yang, X.D., Fan, P.Z., Han, S.S., Zhang, Z.Q. & Xu, Z.Z. (1999). X-ray emission from fs laser interaction with solid targets. *Chinese J. Lasers* **26**, 60–64.

Miyazaki, K. & Takada, H. (1995). High-order harmonic generation in the tunneling regime. *Phys. Rev. A.* **52** 3007–3021.

Nagata, Y., Midorikawa, K., Kubodera, S., Obara, M., Tashiro, H. & Toyoda, K. (1993). Soft-X-ray amplification of the Lyman-α transition by optical-field-induced ionization. *Phys. Rev. Lett.* **71**, 3774–3777.

Sailaja, S., Arora, V., Kumbhare, S.R., Naik, P.A., Gupta, P.D., Fedin, D.A., Rupasov, A.A. & Shikanov, A.S. (1998). A simple XUV transmission grating spectrograph with sub-angstrom resolution for laser-plasma interaction studies. *Meas. Sci. Technol.* **9**, 1462–1468.

Schriever, G., Leben, R., Naweed, A., Mager, S., Neff, W., Kraft, S., Scholze, F. & Ulm, G. (1997). Calibration of charge coupled devices and a pinhole transmission grating to be used as elements of a soft X-ray spectrograph. *Rev. Sci. Instrum.* **68**, 3301.

Sigel, R., Tsakiris, G.D., Lavarenne, F., Massen, J., Fedosejevs, R., Eidmann, K., Meyer-Ter-Vehn, J., Murakami, M., Witkowski, S., Nishimura, H., Kato, Y., Takabe, H., Endo, T., Kondo, K., Shiraqa, H., Sakabe, S., Jitsuno, T., Takaqi, M., Nakai, S. & Yamanaka, C. (1992). Experimental investigation of radiation heat waves driven by laser-induced Planck radiation. *Phys. Rev. A.* **45** 3987–3996.

Wang, C.K., Kuang, L.Y., Wang, Z.B., Cao, L.F., Liu, S.Y., Ding, Y.N., Wang, D.Q., Xie, C.Q., Ye, T.C. & Hu, G.Y. (2008). Phase-type quantum-dot-array diffraction grating. *Rev. Sci. Instrum.* **79**, 123502.

Wang, C.K., Kuang, L.Y., Wang, Z.B., Liu, S.Y., Ding, Y.K., Cao, L.F., Förster, E., Wang, D.Q., Xie, C.Q. & Ye, T.C. (2007). Characterization of the diffraction properties of quantum-dot-array diffraction grating. *Rev. Sci. Instrum.* **78**, 053503.

Yang, J.M., Ding, Y.N., Zhang, W.H., Zhang, J.Y. & Zheng, Z.J. (2003). Precise measurement technology of soft-x-ray spectrum using dual transmission grating spectrometer. *Rev. Sci. Instrum.* **74**, 4268.

Zeng, G.M., Daido, H., Murai, K., Kato, Y., Nakatsuka, M. & Nakai, S. (1992). Line X-ray emissions from highly ionized plasmas of various species irradiated by compact solid-state lasers. *J. Appl. Phys.* **72**, 3355.